Submitted to ApJ

Formation of a proto-quasar from magnetized accretion flows

A. MANGALAM
Inter University Centre for Astronomy and Astrophysics
Post Bag 4, Ganeshkhind, Pune 411 007, INDIA
Internet: mangalam@iucaa.ernet.in

Subject headings: accretion, accretion disks—black hole physics—cosmology:theory—galaxies:formation—galaxies:magnetic fields—galaxies:quasars:general—stars:supernovae:general

ABSTRACT

We present a detailed model for the formation of massive objects at the centers of galaxies. We take into consideration supernovae heating and obtain the conditions of gas loss. Its consequences for the allowed mass range of the halo is calculated and parameterized in terms of the spin parameter, λ_v, the redshift of collapse, z_c, the fraction of baryons in stars, f_*, and the efficiency of supernovae, ν. It is seen that enough gas is retained to form massive dark objects and quasars even for moderately massive halos but a decline is expected at low redshifts. Subsequently, a gaseous disk forms with a radial extent of a kpc, spun up by tidal torques and magnetized by supernovae fields with fields strengths of $10 - 100\mu G$. In a model of a self-similar accretion flow in an initially dominant halo, it is shown that for typical halo parameters, about $10^8 M_\odot$ accretes via small magnetic stresses (or alternatively by self-gravity induced instability) in 10^8 years. A model of a self-gravitating evolution of a compact magnetized disk ($r_0 \lesssim 100$ pc), which is relevant when significant fraction of the disk mass falls in, is also presented and it has a rapid collapse time scale of a million years. The two disk solutions obtained here can be adapted to other prescriptions of viscosity and have applications to other contexts like protostellar disks as well. Implications of this work for dwarf galaxy formation and a residual large scale seed field are also discussed.

1. Introduction

There seems to be increasing evidence that supermassive black holes are at the centers of galaxies. Dynamical searches indicate the existence of massive dark objects (MDOs) in eight systems and their masses range from $10^6 - 10^{9.5} M_\odot$ (Kormendy & Richstone 1995). Although this

and the efficiency of supernovae, ν. Subsequently, the gas in these halos cools before it can escape and a disk forms with a radial extent of about a kpc, containing fairly strong magnetic fields from the supernovae expulsions as shown in §4. We argue in §5.1 that the most likely form of angular momentum transport is via magnetic stresses in the background potential of the halo. The accretion rate estimated turns out be significant. Accretion due to gravitational instabilities is another possibility that is examined in §5.3. A detailed time-dependent treatment of the evolution of such disks in an initially dominant halo is worked out in §6 which confirms the estimated rapid accretion rate of about a $M_\odot$ yr^{-1} into a compact central region. Finally, a self-gravitating magnetized disk solution for this central object that collapses in 10^6 yrs, is presented in §7 . A summary and discussion is presented in §8 and the conclusions in §9.

2. The spherical model

A particularly simple and useful version of the spherical model below assumes that the matter distribution is symmetric about a point and is a pressureless fluid. The shell enclosing mass of the overdense region, $\mathcal{M}$, initially expands with the background universe, slows down, reaches a maximum radius before it turns around, and collapses. The collapse proceeds until a time when it reaches virial equilibrium. For an average density contrast, δ, and using the fact that the background density, $\rho_b \propto t^{-2}$ for a flat cosmological model, one can make the following estimates of the typical parameters of the collapsed object (Padmanabhan & Subramanian 1992, Padmanabhan 1993, Peebles 1980)

$$\begin{aligned}
\rho_0 &= 9.1 \times 10^{-30}\ \Omega\ h_{70}^2 \mathrm{g\ cm}^{-3} \\
\tau_0 &= 0.94 \times 10^{10} h_{70}^{-1}\ \mathrm{yr} \\
r_v &= r_t/2 = (78/\delta_0)\ \mathcal{M}_{10}^{1/3}\ h_{70}^{-2/3} \mathrm{kpc} \\
\tau_c &= 2.19\ \tau_0/\delta_0^{2/3} \\
\delta_0 &= (3\pi/2)^{2/3}\ (1+z_c) = 1.686\ (1+z_c) = 1.062\ (1+z_t),
\end{aligned} \tag{1}$$

where ρ_0 and τ_0 are the current values of the comoving density and time, the subscripts t and c indicate turn around and collapse values, and r_v is the radius of virialization. For a given model of the cosmological evolution of the initial density perturbation, one obtains values for δ_0 or alternatively one can specify the collapse redshift. As an example, $z_t = 6.3$ corresponds to $z_c = 3.6$ and a δ_0 =7.8. We take $\Omega_b = 0.1\ h_{70}^{-2}$ and the mass in baryons, M_9, in units of $10^9 M_\odot$, is related to the total mass by

$$M_9 = \frac{h_{70}^{-2}}{\Omega}\ \mathcal{M}_{10} \equiv \frac{f_b}{0.1}\ \mathcal{M}_{10}. \tag{2}$$

The baryonic mass, M_9, will fuel a black hole, after it has formed, at a rate limited by the Eddington luminosity. If the accretion proceeds at a tenth of this rate, then the luminosity in units of 10^{45}ergss^{-1} is

$$L_{45} = 1.3\ \mathrm{m}_{h8}, \tag{3}$$

C0. Following earlier work (eg. White & Rees 1979, Rees & Ostriker 1977, Silk 1977), we state the condition that a luminous core can form in a halo

$$t_c < t_d \tag{8}$$

where t_c is the cooling time and t_d is the dynamical time. The heating process by was examined in some detail by Dekel & Silk (1986, DS) in the context of dwarf galaxies; they found the condition of gas loss amounted to the virial velocity being below a certain critical velocity. We find that an additional condition for gas loss is necessary, namely, that the cooling time for the hot gas should be smaller than the escape time of the gas. At a time, t_f, when the hot gas in supernovae shells significantly fills up the volume in consideration, the following constraints should be satisfied-

C1. As given by Dekel & Silk (1986), the effective heat input by supernovae is

$$E_{sn}(t_f) \geq \frac{1}{2} f_g \mathcal{M} v_c^2 \tag{9}$$

where f_g is the gas fraction in the total mass and v_c is the circular (or virial) velocity in the halo.

C2. In addition, the time for the hot gas to cool should be longer than the escape time, t_e (to be defined later) of the system

$$\frac{E_{sn}}{\dot{E}} > t_e. \tag{10}$$

In order to quantify these physical constraints, we have to calculate E_{sn}, the effective heat input by supernovae. The standard evolution of a supernova remnant goes through two phases- adiabatic and radiative. In the adiabatic phase (Sedov-Taylor), the radiation loss is negligible and the time at which the shock front radiates about three-quarters of its initial energy is given by DS as

$$t_{rad} \approx 1.4 \times 10^5 \; n^{-1/2} \text{ yr}, \tag{11}$$

where n is the ambient hydrogen number density in cm^{-3}. As a result, the input into the gas equals the initial energy minus the radiative losses in the adiabatic phase and subsequently for later times, the gas is cooled by expansion. The cumulative energy input from the supernovae at a given time, t, will be dominated by those that have exploded within a time t_{rad} before t. The star formation rate is taken to be a constant and is approximately, $f_* M/t_d$, where f_* is the baryonic mass fraction in stars and further, it is assumed that the star formation abruptly ends at $t = t_d$. The IMF of the solar neighborhood gives rise to one supernova per 200 $M_\odot$ of newly formed stars. If ν_{200} is the number of supernova explosions per $200 M_\odot$ of newly formed stars[1]

[1]An analytic fit to the IMF (eqn(1.3.10), Shapiro & Teukolsky, 1983) which is based on Bahcall & Soniera (1980), yields the ratio of the number of objects in the mass range $5 < M/M_\odot < 30$ to the total mass in all the stars with a cutoff at 0.1 $M_\odot$ to be 5×10^{-3} per solar mass; this we have adopted as a fiducial value of the number of supernovae per solar mass of newly formed stars.

where eqn(16) and the density of the gas, $M(1-f_*)/(4\pi R^3) = 1.4\ n\ m_p$ was used. Since the star formation shuts off at $t = t_d$, the maximum value of the ratio of the total shell volume to gas volume is $F(t > t_d) = 10\ (4f_*/(1-f_*))\ \nu_{200}\ n^{-1/5}$. This implies that the filling factor of the supernovae shells in the galaxy will be weakly dependent on number density. One can take into account the porosity (which can be thought of as the complement of the probability that a given point in the volume is outside the $N = \nu_{200}\ f_*\ M_9\ (5 \times 10^6)$ remnants of fractional volume, $q = F(t)/N$, occupied by one shell) by $Q = 1-(1-q)^N$, where Q is the filling factor which is well approximated in the Poisson limit of large N by the formula,

$$Q(t) = 1 - \exp\left(-F(t)\right). \tag{18}$$

It is clear that Q at large times is close to 1 (and nearly independent of density) and the hot gas fills the volume. In order to estimate the total energy input into the medium in eqn(12), we calculate the time, t_f, when $Q \approx 1, F(t_f) = 3$ which leads to $t_f = F(t_f)t_d/F(t_d) \simeq 0.3t_d = 30\ t_{rad}$.

3.2. Gas loss criteria

The solution leads to $f(t_f) \approx 3$. So the energy input into gas from supernovae works out to be

$$E_{sn}(t_f) = 3 \times 10^{55}\ \frac{f_*}{0.2}\ \frac{f_b}{0.1}\ \nu_{200}\ \mathcal{M}_{10}\ \text{ergs} \tag{19}$$

The escape energy is given by

$$\frac{1}{2}\ f_g\ \mathcal{M}\ v_c^2 = \frac{1}{2}\ \frac{G f_g \mathcal{M}^2}{r_v} = 4 \times 10^{55}\ \frac{(1-f_*)}{0.8}\ \frac{f_b}{0.1}\ \frac{\mathcal{M}_{10}^2}{x_v}\ \text{ergs} \tag{20}$$

where

$$v_c = 0.7 \times 10^7 \sqrt{\mathcal{M}_{10}/x_v} \text{cm s}^{-1} \tag{21}$$

is the virial velocity. As a result the condition C1 for gas removal can be written as

$$\frac{v_{sn}^2}{v_c^2} = \frac{3f_*}{1-f_*}\ \frac{x_v}{\mathcal{M}_{10}}\ \nu_{200} > 1 \tag{22}$$

where $v_{sn}^2 = 2E_{sn}/(f_g\mathcal{M})$ where $f_g = 1 - f_b(1-f_*)$ is the gas fraction in the halo mass not converted to stars. It is clear that enhancing the star fraction increases the energy input into a smaller gas fraction and hence v_{sn}^2 is a monotonically increasing function of f_*. Also, halos of the same mass had deeper potential wells in the past which trap the gas better. Similarly, more massive halos clearly have deeper wells and gas loss is less likely as seen from eqn(22).

In appendix A, we calculate the difference in gravitational binding energies in the initial configuration of an isothermal halo and a final one consisting of an exponential gaseous disk in a halo consisting of stars and dark matter. The gas taken to be roughly near the virial temperature,

$$T_v = \frac{G\ \mathcal{M}\ \mu\ m_p}{3\ k_b\ r_v} = \frac{\mathcal{M}_{10}}{x_v}\ 0.9 \times 10^5\ K \tag{23}$$

where the effective dynamical timescale at $\delta = 1$ is taken to be t_d and $t_e(1) = 0.418 t_d$, so that the curve C2 is continuous with C0. This is seen the cooling diagram, presented in Fig 2, where the number density of hydrogen in the halo, $n(\mathrm{cm}^{-3}) = \mathcal{M}_{10}/(130 x_v^3)$, is plotted against the virial temperature, T_v and shows the curves given by C0, the lower curve, C1, the vertical line, and C2 which is the upper curve in the region to the left of C1. The cosmological parameters were set to $h_{70} = 1, \Omega = 1$, and $f_b = 0.1$ and the halo parameters were chosen to be $\lambda_v = 0.075, f_* = 0.2$, and $\nu_{200} = 4$. The shaded region indicates the halos that have collapsed but star formation has induced gas loss and they ultimately resulted in gas poor systems. The halos above this region retain the gas that could form the massive central black holes. The corresponding range in mass for a given redshift is shown in Fig 3, for the choices of the parameters, $\nu_{200} = 4$, the supernova efficiency, and $f_* = 0.2$, the fraction of baryons in stars. Clearly for large redshift, the mass range increases and this is due to the deeper potential well which can retain the gas better. There is a crucial question of whether all the gas is retained or if some fraction is lost in a wind. A supernova efficiency in the halo of

$$\nu_{200} \frac{4 f_*}{1 - f_*} \gtrsim 60 \sqrt{\mathcal{M}_{10}/x_v^3} = 4.3(1 + z_c)^{3/2} \tag{30}$$

from eqn(29), would be required to drive winds that would result in mass loss and this is considerably more than the corresponding estimates in our galaxy, for $z_c \gtrsim 2$. If the stars form after the disk forms, the cooling rate in the disk would be given by

$$\dot{E}_d = 3 \times 10^{44}\ \Lambda_{23} \left(\frac{f_b}{0.1}\right)^2 \mathcal{M}_{10}^2\ x_d^{-3}\ (1 - f_*)^2\ \frac{r_d}{H}\ \mathrm{ergs\ s}^{-1} \tag{31}$$

and the cooling time would reduce by a factor of a thousand corresponding to enhanced density. Although only the cosmological abundance of $[Fe/H] = -4$ was used, the supernovae explosions will also enhance line cooling from metals injected into the medium; this would reduce the cooling time estimated here.

4. Magnetization of the disk

In the large number of the halos which trap the gas as given by the conditions C0–C2, a gaseous disk forms with a radial extent given in §2.1. Further, it was seen in §3.1 that the supernovae shells fill the core volume at the time of star formation, and the small scale magnetic fields are dragged with the gas as it settles into a the disk. Now, we consider the question of whether the field strength is large enough to provide a significant viscous stress. We take the gas to be initially dominated by the gravity of the dark halo and assume the following logarithmic potential (Binney & Tremaine 1987, eqn (2-54)) that obeys the flat rotation curve

$$\Phi(r, z) = v_c^2\ \ln(r_0^2 + r^2 + (z/q_\phi)^2) \tag{32}$$

where r_0 is the radius of a compact region, $q_\phi \leq 1$ and v_c is defined in eqn (21). If the vertical equilibrium was a result of balance between vertical gradient in the total pressure, $P = \zeta c_s^2 \rho$

unlikely to pervade the volume, and the major contribution would be from supernovae. Although the number of massive stars are of the same order as the number of supernovae using the Salpeter IMF (estimated by integrating the mass range above $10M_\odot$; see the footnote in §3), the smaller fluxes of the wind ($\sim B_s R_*^2$ where R_* is the radius of the star) render the effective field strength to be weak. *The key point here, is that for typical values of the halo parameters, B_{sn} is about $10^{-4} - 10^{-5}$ G which is a factor of 10–100 higher than the value in our galaxy ($V_d = 6 \times 10^{11}\mathrm{pc}^3, N \sim 3 \times 10^8, B_{sn} = 3\mu G$) due to a smaller value of V_d/N of the supernovae shells.*

5. Accretion to a compact region

Here we consider different viscosity prescriptions, namely direct magnetic stress, the phenomenological α viscosity (Shakura & Sunyaev 1973) derived from magnetic fields, and angular momentum transfer mediated by self-gravity induced instabilities, and calculate the corresponding accretion timescales. The time dependent disk accretion is described by the conservation of mass, radial momentum (where all other forces except gravity are neglected, and $v_r/v_\phi \ll 1$) and angular momentum

$$r\partial_t \Sigma = -\partial_r(r\Sigma\, v_r) \tag{39}$$

$$\omega^2 = (1/r)\partial_r \Phi \tag{40}$$

$$\Sigma v_r \partial_r(r^2\omega) = 1/r\ \partial_r(r^2 \Pi_{r\phi}), \tag{41}$$

where $\Sigma(r,t)$ is the surface density, Φ is the gravitational potential and $\Pi_{r\phi}$ is the vertically integrated stress. Taking r_c as the inner radius of the disk flow and the outer edge of the compact region while

$$\omega(r) = \frac{\omega_0}{\sqrt{1+(r/r_0)^2}}. \tag{42}$$

By integrating eqn (41), we obtain for steady flow

$$\dot{M}\omega\left(1 - \frac{r_0^2\omega_0}{2r^2\omega}\right) = 2\pi\Pi_{r\phi}. \tag{43}$$

The viability of the various alternatives for the viscous stress can be assessed by estimating the accretion rates. In the initial phase of accretion the potential is dominated by the halo as calculated in §6 while in the later phase self-gravity dominates and the resulting flow is calculated in §7.

5.1. Magnetic Stress

We consider now the form of the stress tensor that is entirely due to magnetic fields. We assume that the magnetic field injected is largely in the form of small scale loops that are frozen

5.2. α viscosity

If a small scale dynamo operates quickly (Kasantev 1967, Kulsrud & Anderson 1992) then it will saturate near equipartition values (as is well known from simulations - Hawley, Gammie & Balbus 1995 and references therein) and an appropriate form of the stress can be described in terms of a prescription of the form $\Pi^{ss}_{r\phi} = -2H\alpha_{ss}P$, where $P = \zeta\rho c_s^2$ is the total pressure, which is proportional to the gas pressure at equipartition. The accretion time scale is expected to be similar to the one obtained earlier. The dependence on the halo parameters can be expressed in the isothermal limit as

$$t_\alpha \sim 2\times 10^8 \text{ yrs } \frac{0.1}{\alpha_{ss}} \left(\frac{4.6}{1+z_c}\right)^{1/2} \frac{0.1}{f_b}\, \mathcal{M}_{10}^{-2/3} \left(\frac{0.8}{1-f_*}\right) \mathrm{m}_{h8}. \tag{50}$$

Note that, although we use a direct magnetic stress in our calculations, we record for comparison, the detailed form of the α prescription here. By assuming that the gas is a polytrope of index γ

$$P\ (\Sigma/2H)^\gamma = K, \tag{51}$$

and using the vertical equilibrium, eqn (34), we obtain

$$\Pi^{ss}_{r\phi} = -\alpha_{ss}PH = -\alpha_{ss}K^{3\gamma/(2-\gamma)}\Sigma^{-3\gamma/(2-\gamma)}\omega^{2(\gamma+1)/(\gamma-2)}. \tag{52}$$

5.3. Gravitational instabilities

Cold, thin rotating discs are known to be unstable and the basic stability criteria was provided by Toomre (1964). For an uniformly rotating isothermal disk (Goldreich & Lynden-Bell 1965) the criteria for local stability is given by

$$Q_T = \frac{c_s\omega}{G\Sigma} \geq 1.06. \tag{53}$$

We find that

$$Q_T = \frac{\pi v_c^2 H}{GM_d} = \frac{\pi}{8}\, \mathcal{M}_{10}^{-1/3} \left(\frac{4.6}{1+z_c}\right)^{1/2} \frac{0.8}{1-f_*}\, \frac{0.1}{f_b}, \tag{54}$$

where the values ($\theta = 1/8, \lambda_v = 0.075$) were assumed. So the disk is unstable to gravitational instabilities and it is possible for angular momentum transport to occur through this process. Lin & Pringle (1987) estimate an effective kinematic viscosity for gravitational instability from $\nu_e = \omega\ell^2$, where the critical shearing length, $\ell = G\Sigma\omega^{-2}$ was taken to be the maximum possible size for the instability. Here we make a more conservative estimate by introducing the parameter, $Q_T^2 < \alpha_g < 1$, into the stress given by

$$\Pi^g_{r\phi} = \alpha_g\, \nu_e\, \Sigma\, r\partial_r\omega = -\alpha_g\, G^2\, \Sigma^3\, \omega^{-2} \qquad \text{if } \ Q_T < 1. \tag{55}$$

The corresponding timescale of accretion is

$$t_g \sim 10^8\, M_\odot \left|\frac{\omega\, \mathrm{m}_{h8}}{2\pi\, \Pi^g_{r\phi}}\right| = 10^8 \text{ yrs } \mathcal{M}_{10}^{1/2} \left(\frac{4.6}{1+z_c}\right)^3 \left(\frac{0.8}{1-f_*}\right)^3 \left(\frac{0.1}{f_b}\right)^3 \frac{0.1}{\alpha_g}\, \mathrm{m}_{h8}. \tag{56}$$

Moreover, if $b > 1$, which is the case for the examples considered here, then $c_1 = 0$. By rearranging terms and integrating, we obtain the following solution

$$g(\xi) = \xi^{(a-c)/b} \left(1 - \xi^{2+\frac{(c-a)}{b}}\right)^{1/(b-1)}. \tag{64}$$

The time constant can be evaluated with $r_s = r_d$ to be

$$t_0 = \frac{\omega}{\Pi_{r\phi}(\Sigma_0, r_d)} \frac{M_d}{2\pi l} = t_a l^{b-1} \frac{M_{d8}}{\mathrm{m}_{h8}}, \tag{65}$$

where t_a is the accretion time scale calculated in §5.1 and §5.3 in the steady case using $\Pi_{r\phi}(M_d/(2\pi r_d^2), r_d)$. The rate at which mass sinks into the center is given by

$$M_c(t) = M_d \left[1 - \left(\frac{t}{t_0}\right)^{-(a+2)\alpha}\right] \tag{66}$$

The accretion time scale which is the time that transpires when a fraction $\epsilon = \mathrm{m}_{h8}/M_{d8}$ of the disk mass falls in is given by

$$\tau_a = t_0 \left((1-\epsilon)^{\frac{-1}{(a+2)\alpha}} - 1\right) = t_a\, l^{b-1} \left((1-\epsilon)^{\frac{-1}{(a+2)\alpha}} - 1\right) \epsilon^{-1} \tag{67}$$

where t_a represents the timescales t_m, t_g or t_α, and indicates that the estimates derived earlier are modified by geometric factors. Now we consider the particular case of magnetic accretion ($a = -1, b = 4/3, c = -1/3, \epsilon = 1/8$, see §5.1 where the value of ϵ is chosen for a typical case where the disk mass, $M_{d8} = 8$, and $\mathrm{m}_{h8} = 1$) which has the solution

$$\alpha = 3/7, \quad \beta = -9/7, \quad \tau_m = 1.01\, t_m, \quad g_m(\xi) = \xi^{-1/2} \left[1 - \xi^{3/2}\right]^3. \tag{68}$$

Similarly, the accretion due to gravitational instabilities ($a = -1, b = 3, c = 2, \epsilon = 1/8$, $M_{d8} = 8$, and $\mathrm{m}_{h8} = 1$, see §5.3) has the solution

$$\alpha = 1/5, \quad \beta = -3/5, \quad \tau_g = 0.54\, t_g, \quad g_g(\xi) = \xi^{-1} \left[1 - \xi\right]^{1/2}. \tag{69}$$

The disk structure of these solutions are shown in Fig. 4. The self-similar solutions of this kind to (57) are known to develop at large times in numerical simulations with a variety of initial conditions (Lin & Pringle 1981).

Now we determine the regime in parameter space where the halo dominated flow can occur. This is given by the condition that at $t = t_0$ and $r = r_d$, the halo dominates self-gravity or

$$\begin{aligned} \frac{v_c^2}{r_d} &> \left.\frac{\mathrm{d}\Phi_d}{\mathrm{d}r}\right|_{r=r_d} \\ \frac{M_h}{r_d r_v} &> \frac{M_d}{l r_d^2} \sum_n \alpha_n^2 J_1(\alpha_n) \int_0^1 J_0(\xi\alpha_n) g(\xi) \xi \mathrm{d}\xi, \end{aligned} \tag{70}$$

7. Disk evolution in a self-gravitating regime

We now examine the evolution of the disk in a gravity field that is entirely due to itself. This flow can occur after sufficient accretion of mass into a compact region of radius r_0; or, alternatively at the time of the formation of the disk if the eqn (72) is not satisfied and $\lambda_v(1-f_g)/f_g \lesssim 0.32$. The problem of self-gravitating accretion flow is complicated by the coupling of Poisson's equation to the momentum and continuity equations. Clearly, its evolution has to be treated differently from the preceding case of a prescribed background potential. A detailed model is deferred to a work in preparation (Mangalam 1999); in this present paper we adopt a simplified approach that is due to Field (1994).

We assume a Mestel (1963) disk where the self-consistent density distribution with potential is entirely due to self-gravity, is of the form

$$\Sigma(r,t) = \frac{v_\phi^2(t)}{2\pi G r}, \tag{75}$$

where the time dependence appears only in the rotational velocity. This is a an interesting disk which is self-consistent, taking into account the most relevant physics although only in a parametric fashion. Taking

$$v_\phi = v_0\,\chi(t) \quad \text{and} \quad r = r_0\,\chi_1(t)\,x \tag{76}$$

where $v_0^2 = GM_c/r_0$, and M_c is the mass out to r_0. We see that by assuming a self-similar evolution of the disk, the mass out to a given x should be independent of t and hence it follows that

$$\chi_1 = \chi^{-2} \quad \text{and} \quad \Sigma = \Sigma_c\,\frac{\chi^4}{x}, \tag{77}$$

where $\Sigma_c = M_c/(2\pi r_0^2)$. From the continuity equation,

$$r\partial_t\Sigma + \partial_r(r\Sigma v_r) = 0 \tag{78}$$

we find

$$v_r = -4\chi^{-3}\dot{\chi} r_0 x. \tag{79}$$

Substituting this and the self-similar forms given above into the angular momentum equation,

$$\begin{aligned} \Sigma\partial_t v_\phi + \Sigma(v_r/r)\partial_r(rv_\phi) &= (1/r^2)\partial_r(r^2\Pi_{r\phi}) \\ -3v_0\Sigma_c\chi^2\dot{\chi} &= \frac{\mathrm{d}}{\mathrm{d}x}\left(x^2\Pi_{r\phi}\right), \end{aligned} \tag{80}$$

we obtain

$$\Pi_{r\phi} = -\frac{3}{2}v_0\Sigma_c r_0\chi^2\dot{\chi}, \tag{81}$$

which is *independent* of x. So far no specific viscosity mechanism has been invoked– the form of $\Pi_{r\phi}$ above is necessitated by the prescription of a Mestel disk. If a magnetic stress is assumed and $\Pi_{r\phi} = -\kappa B^2 H/(2\pi)$, where κ is a factor of order unity and B is given by the vertical balance of

4. A general solution for a self-similar and time dependent accretion flow for a viscous stress of the form $\Pi_{r\phi} \propto \Sigma^b r^c$ in a prescribed potential, $\omega \propto r^a$, was obtained in §6. This was applied to the specific cases of magnetic accretion, eqn(68) and and gravitational instabilities, eqn(69). The structure of the resulting disk is shown in Fig. 4 and the timescales are within geometric factors of their estimates. The disk eventually becomes fully Keplerian. The condition of halo dominated flow is given by eqn(72) and the transition to a self-gravitating flow is given by eqn(74). This solution is valid for dominant halos in the initial stages for the outer parts, $y > 0.1$, oustide a Keplerian compact region for up to time when a fraction of the disk mass, $\epsilon \sim 0.3$, falls in (see Fig 5).
5. A self-gravitating Mestel disk (based on Field 1994) that is spinning up as it is collapsing self-similarly, is described in §7. We apply this to a compact region where the pressure is assumed to be due to magnetic fields. The time scale of collapse turns out to be the rotation time of the outer radius, which is a few million years.

We now discuss some of the issues involved:

Supernovae feedback

In a pioneering work, DS, showed that with a model of protogalactic gas in a halo reproduces the observed relations very well with an initial CDM model. Further, the condition for gas loss was given by the condition that the energy input from supernovae is more than the binding energy, C1 and the cooling condition for gas contraction and star formation. In this work, we specify an additional necessary condition, C2, that the escape time be shorter than the cooling time. As indicated in Fig. 2, this restricts the gas loss to the halos in the shaded region. The exact shape and location of the region is subject to the choice of parameters (ν, f_*), but the key point made here is that the entire region to the left of C1 cannot be considered as a gas loss zone, even if heating by background UV photons were included. It is worth investigating this question in more detail by simulations that include the hydrodynamics and cooling of the hot gas. Based on this study, one can conclude that most of the dwarf galaxies involved efficient conversion of stars or high efficiency of supernovae, since that would place curve C2, higher on the cooling diagram accounting for the prediction of the location of the dwarf galaxies made by DS. The constraints imposed here, however, account for the presence of black hole systems on the left of C1 (and above C2). It also explains a sharp decline in quasars at epochs later than $z = 2$.

Magnetic field strength in supernovae shells

In estimating the field strength B_{sn} in §4, all the shells were assumed to have 10^{-4} G when they are young (size of 0.8 pc) and flux freezing was used to estimate the values at a given size. This field has been measured in the Crab nebula and in other young supernova remnants like Tycho, Kepler and Cas A, the field strength in the shell is inferred to be $10^{-3} - 10^{-4}$ G (Strom & Duin 1973, Henbest 1980, Anderson et al. 1991). Simulations by Jun & Norman (1996), show local turbulent amplification by Rayleigh-Taylor and Helmholtz instabilities but claim overall

occurs halting a direct collapse to relativistic scales and suggested that low spin systems could form supermassive seeds of disk or star geometry which would contract under radiative viscosity. The picture proposed here is that direct magnetic stress or gravitational instabilities in the disk can transport matter into a compact region on a dynamical timescale. The scheme of gravitational instabilities hinges on $Q_T < 1$ in the disk whereas the direct magnetic stress depends on the supernova efficiency and field expulsion. The presence of high magnetic energy density from MHD turbulence has been invoked to explain high velocity dispersions of H I clouds in galactic disks (Sellwood & Balbus 1999).

Angular momentum in the inner region ($\lesssim 1$ pc) is likely to be more complicated due to radiation pressure that would prevent collapse. The model of self-gravitating magnetized collapse in §7 was illustrative of the timescale involved but a detailed model for the inner region that takes into account radiation pressure, radiative viscosity and evolution of the field is required. If dynamo action takes place within the compact region ($\lesssim 100$ pc), the exponentiation timescale in the linear regime will be of order $1/\omega(r_0) \sim 10^6$ yrs. The residual large scale seed field ($\sim 10^{-7}G$) from supernovae can be amplified to dynamical values (mG) in 10^7 years and the e-folding timescale for magnetic braking is $r_0/v_A \sim (M(r_0)/r_0)^{1/2}/B = 10^6$ yrs corresponding to this field strength.

9. Conclusions

In this work, a semi-analytic model of quasar formation was attempted which captures the essential details of star formation with supernovae feedback and angular momentum transport via magnetic fields. Based on the novel results in this work (as summarized in §8), and for the relevant range in parameter space, it is seen that a $10^{10}M_\odot$ cloud at z of 8 can collapse to form a gaseous disk in the dark halo by z of 4.8 and about $10^7 - 10^8 M_\odot$ of gas (which is 0.01–0.1 of the total disk mass) accretes into a $r_0 \lesssim 100$ pc region in a fast timescale of 10^8 yrs. The magnetic stress from supernovae can be significant in the disk and is preferred over other possibilities as observational evidence exists for star formation, and large scale fields at $z \sim 2$. A dynamo generated field can also play a prominent role in bipolar outflows and accretion disks that are associated with quasars.

The solution to the non-linear diffusion equation presented in §6 can be applied in other contexts, eg. protostellar disks. As a part of future work it is planned to investigate a detailed model of the inner region using a simulational approach, the impact of the restriction on the mass range of black hole hosts ($\mathcal{M} - z$) by supernovae feedback on the quasar luminosity function and dwarf galaxies, and the strength of the large scale seed field.

I thank K. Subramanian whose suggestions and encouragement improved this work considerably. I also thank C. J. Jog, F. K. Lamb, B. Nath, B. Roukema and P. J. Wiita for valuable discussions. I acknowledge support from the NSF grant AST 96-18524 at the University of Illinois at Urbana-Champaign where this work was begun.

Binney J., & Tremaine, S. 1987, Galactic Dynamics, Princeton: Princeton University Press

Bisnovatyi-Kogan, G. S., Ruzmaikin, A. A., & Sunyaev, R. A. 1973, Soviet Ast., 17, 137

Blandford, R. D., & Rees, M. J. 1992, in Testing the AGN Paradigm, ed. Holt, S. S., Neff, S. G., Urry, C. M. (NewYork: Am. Inst. Phys.), 3

Chevalier, R. A. 1974, ApJ, 1988, 501

Dekel, A., & Silk, J. 1986, ApJ, 303, 39 (DS)

Field, G. B. 1994, in Cosmical Magnetism, ed. Lynden-Bell, D. (Cambridge: Institute of Astronomy, Cambridge)

Ford, H. C. et al. 1994, ApJ, 435, L27

Jun, B.-I., & Norman, M. L. 1996, ApJ, 465, 800

Goldreich, P., & Lynden-Bell, D. 1965, MNRAS, 130, 125

Haenelt, M. G., & Rees, M. J. 1993, MNRAS, 263, 168

Hamann, F., & Ferland, G. 1992, ApJ, 391, L53

Hawley, J. F., Gammie, C. F., & Balbus, S. A. 1995, ApJ, 440, 742

Heavens, A. F., & Peacock, J. A. 1988, MNRAS, 232, 339

Henbest, S. N. 1980, MNRAS, 190, 833

Kasantsev, A. P. 1968, Sov. Phys. -JETP, 26, 1031

Keohane, J. W., Gotthelf, E. V., & Petre, R. 1998, ApJ, 503, L175

Kormendy, J., & Richstone, D. O. 1995, ARA&A, 33, 581

Kronberg, P. P., Perry, J. J., & Zukowski, E. L. H. 1992, ApJ, 387, 528

Kulsrud, R., & Anderson S. W. 1992, ApJ, 396, 606

Larson, R. B. 1974, MNRAS, 169, 229

Lin, D. N. C., & Pringle, J. E. 1987, MNRAS, 607

Loeb, A., & Rasio F. A. 1994, ApJ, 432, 52

Mangalam, A. 1999, in preparation

Mestel, L. 1963, MNRAS, 126, 553

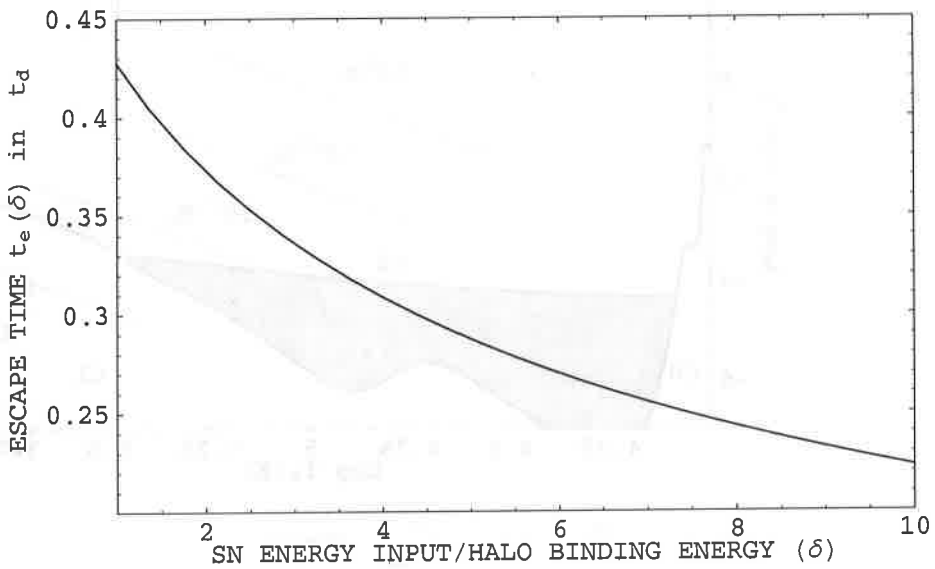

Fig. 1.— The dependence of the escape time of the hot gas, in units of the dynamical time in the halo which is defined as one-quarter oscillation period, on $\delta = v_{sn}^2/v_c^2$, the supernovae energy input in units of the halo binding energy. A factor of 10 in the heat input reduces the escape time, t_e, by factor of 2.

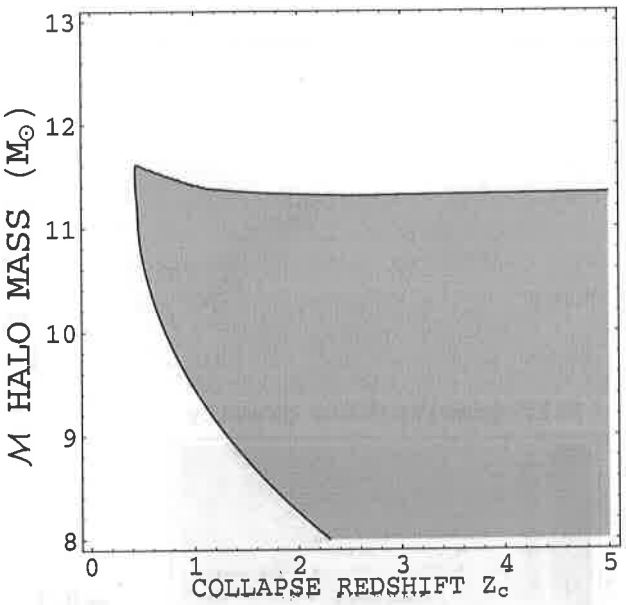

Fig. 3.— The halos in the shaded region in the $\mathcal{M}_{10} - z_c$ space can trap the gas; the parameters chosen are $f_* = 0.2, \nu_{200} = 4$, and $\lambda_v = 0.075$.

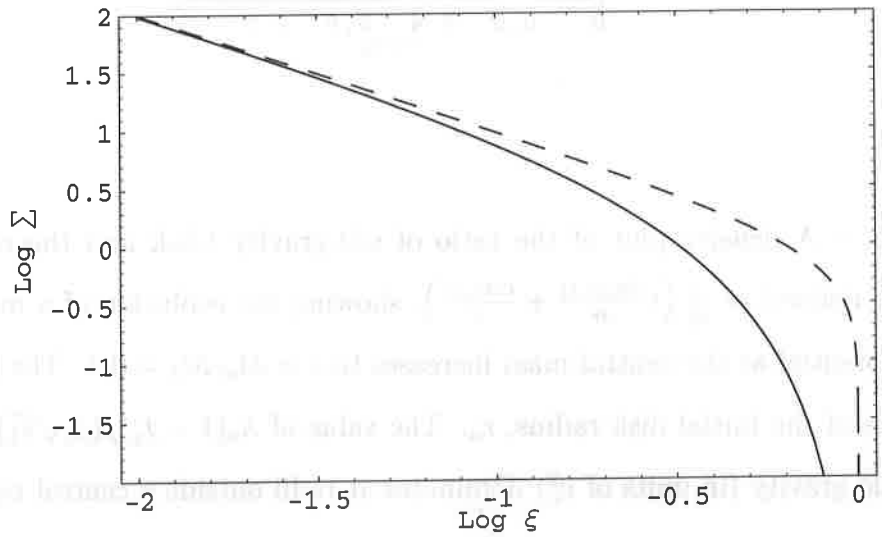

Fig. 4.— The structure $g(\xi)$ of the self-similar disk, $\Sigma = \Sigma_0 \left(\frac{t}{t_0}\right)^{\beta} g(\xi)$ where $\xi = r/r_f, r_f = r_s \left(\frac{t}{t_0}\right)^{\alpha}$. The magnetic solution, $g_m(\xi) = \xi^{-1/2}\left[1 - \xi^{3/2}\right]^3$ is shown by a solid line, and the solution of the disk with gravitational viscosity, $g_g(\xi) = \xi^{-1}\left[1 - \xi\right]^{1/2}$, is shown by a dashed line.